Mathematical Modelling and Control

http://www.aimspress.com/journal/mmc

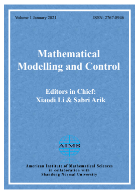

MMC, 2(4): 176–184
DOI:10.3934/mmc.2022018
Received: 30 August 2022
Revised: 05 October 2022
Accepted: 30 October 2022
Published: 16 December 2022

Research article

Vehicle kinematic and dynamic modeling for three-axles heavy duty vehicle

Yongming Li[1,*], Shou Ma[2], Kunting Yu[3] and Xingli Guo[4]

[1] College of Science, Liaoning University of Technology, Jinzhou 121000, China

[2] School of Electrical Engineering, Liaoning University of Technology, Jinzhou, 121000, China

[3] Navigation College, Dalian Maritime University, Dalian 116026, China

[4] Technology Center, Liaoning Aerospace Linghe Automobile Co., Ltd, Chaoyang,122000, China

* **Correspondence:** Email: l_y_m_2004@163.com.

Abstract: Under complex conditions, the vertical, lateral and longitudinal dynamics of vehicles have obvious coupling and interaction. This paper aims to provide a suitable driver cab and a vehicle model for the study of vehicle coupling dynamic performance. In modeling the cab and body kinetic equation, two shock absorbers are considered in the front axle suspension system. In addition, the vertical, roll and pitch motion of the diver cab, vehicle body, the vertical and roll behavior of three wheel axles, the pitch angles of the left and right balancing pole on rear suspension, and roll angle the of each tire are considered. Finally, based on the above coupled motion characteristics, a diver cab and a vehicle model for three-axles heavy-duty vehicle with 26 degrees of freedom (DOF) are proposed.

Keywords: three-axles heavy-duty vehicle; 26 degrees of freedom model; coupling dynamic performance

1. Introduction

During the vehicle movement, the performance of the vehicle is affected by various vehicle structures and functions, such as power steering system, suspension system, braking system, etc. Moreover, in complex and high-speed environment, the vehicle's vertical, roll and pitch displacements contain a strong coupling relationship. Therefore, considering the motion and coupling characteristics of vehicle structures is meaningful to investigate vehicle dynamics. On the basis of geometric structure parameters of vehicle system and the nonlinear characteristics of shock absorber and leaf spring, the authors in [1] establish a nonlinear dynamic model for heavy vehicle. The correctness of the dynamic model is verified by testing the vertical acceleration data of the driver's seat, front wheel, middle wheel and rear wheel. To investigate the longitudinal driving behaviors of vehicle dynamics in the platoons, by taking the acceleration capability of heavy-duty vehicle into account, numerous heavy-duty vehicle platoon models are proposed [2–10]. Furthermore, by considering the lateral and longitudinal displacement characteristics of the vehicle, [11] represents a 2 DOF model of the vehicle and two diver cab models with time delays. In order to further describe the vehicle dynamics characteristics, in accordance with the two driver cab models in [11]. [15] and [16] further investigate the nonlinear lateral dynamics of a 2 DOF vehicle model. Based on longitudinal vehicle dynamics and by analyzing the dynamic of engine, torque converter, tire and capacitor pack, the authors of [17] present a dynamic model for a heavy-duty vehicle.

On the other side of research, the above mentioned vehicle models are mostly used to evaluate vehicle lateral and longitudinal dynamics characteristics, the influence of vehicle lateral and yaw dynamics characteristics are not considered enough. In practice, the tires not only provide horizontal and vertical forces to the vehicle, but also give vertical forces to the suspension system, especially in complex driving situations such as lane changes, cornering, or obstacle avoidance. In these cases, the vehicle's vertical, roll, and pitch dynamics are clearly coupled with lateral and yaw motion. Due to large inertia, high center of gravity and high roll center, heavy vehicles have poor stability when entering a turn or lane change, and the three-way coupling effect is large. Therefore, it is necessary to establish a three dimensional coupled vehicle model and study the influence of steering process on vehicle dynamics. More recently, more and more works focus on the coupling property of the vehicle. To reflect the steering influence on the overall response of the vehicle, [18] designs a novel 4 DOF hydraulic power steering (HPS) system. Simultaneously, [18] develops a 24 DOF model by taking the HPS system, the steering hand wheel angle, rack displacement, and hand wheel angles into account. According to the nonlinear characteristics of suspension damping and tire stiffness, [19] establishes a nonlinear three-way coupled lumped parameter model, and an improved nonlinear delay preview driver model was proposed based on [11], which was connected with the TCLP model to form a driver-vehicle closed-loop system. [20] establishes a complete vehicle model of a heavy truck, which not only investigates the nonlinear characteristics of suspension damping and tire stiffness, but also contains a modified preview driver model with nonlinear time delays to calculate the right front wheel steering angle for driving the vehicle along the desired route. In this paper, the kinematics and dynamics equations of cab and body are established by analyzing the three-way coupling effect of cab and body, as well as the dynamic characteristics of tire and suspension. Firstly, the dynamic relation of the tyre with deflection angle is introduced. Secondly, the coupling dynamics equation of cab was established by analyzing the three-way coupling effect of cab. Then, considering the dynamic characteristics of the vehicle suspension, the three-way coupling dynamic equation of the vehicle body is established. Finally, the kinematic and dynamic equations of cab and body are established based on the dynamic characteristics of tire and suspension and the Euler rotation theorem.

2. Nomenclature

Table 1. The symbols of the heavy-duty vehicle.

Definition	**Symbol**
forward traction (lateral traction) of the $i-th$ tire	$F_{xi}(i=1,\cdots,6)(F_{yi})$
steering angle of the $i-th$ wheel	δ_i
steering angular speed of the front axle tires	ω_t
transverse (longitudinal) component of $i-th$ tire along the coordinate system $\{B\}$	$F_{Xi}(F_{Yi})$
suspension force, damping coefficient and spring constant of the $j-th$ spring between cab and body	F_{cj}, H_{cj} and K_{cj} $(j=1,2,3,4)$
vertical displacement of the cab (body)	$z_c(z_b)$
pitching angle of the cab (body)	$\varphi_c(\varphi_b)$
roll displacements of the cab (body)	$\phi_c(\phi_b)$
longitudinal distance between origin of coordinates $\{C\}$ and cab rear (front) spring	$l_5(l_6)$
the distance between the origin of coordinates $\{C\}$ and $\{B\}$	l_4
the angle between the origin of coordinate $\{B\}$ and the sprung mass bar center of suspension	φ_0
transverse distance betweencab front spring and rear spring	b_c
resultant force of the cab inthe direction of axes X_C, Y_C and Z_C	F_{xc}, F_{yc} and F_{zc}
resultant moment of the cab in the direction of axes X_C, Y_C and Z_C	N_{xc}, N_{yc} and N_{zc}
total mass of the vehicle, cab and body	m_s, m_t and m_b
velocity vectors of the cab in the coordinate system $\{C\}$ and $\{B\}$	u_c, v_c and w_c, u_b, v_b and w_b
roll angle rate, pitch angle rate and yaw angle rate of the coordinate system $\{C\}$ and $\{B\}$	p_c, q_c and r_c, p_b, q_b and r_b
vertical and transverse distance from the origin of $\{C\}$ and $\{B\}$ to the center of gravity of cab	h_{os} and e_{os}, h_{ob} and e_{ob}
moment of inertia of a vehicle about axle X_C, Y_C, Z_C, X_B, Y_B and Z_B	I_{xxc}, I_{yyc} and I_{zzc}, I_{xxb}, I_{yyb} and I_{zzb}
moment of inertia of the cab about the axis X_C and Y_C (X_B and Y_B)	I_{xxsc} and I_{yysc} $(I_{xxsb}$ and $I_{yysb})$
integral of the product of the X_C and Y_C(X_B and Y_B) deviation of an area element in a vehicle	$I_{xzc}(I_{xzb})$
compression displacement of the $j-th$ spring between cab and body	x_{cj}
cab center of gravity (body center of gravity) to cab front and rear spring transverse distance	l_7 and l_8 (l_{15} and l_{16})
transverse (longitudinal) distance of cab center of gravity to set 1, set 2 and set 3 tires	l_9, l_{10} and l_{11} (l_{12}, l_{13} and l_{14})
distance between the front axle and the rear axle in a suspension system	l_3
resultant force of the cab in the direction of axes X_B, Y_B and Z_B	F_{xb}, F_{yb} and F_{zb}
suspension force, damping coefficient and spring constant of the $j-th$ spring between the front axle or rear axle and the body of the suspension system	F_{sj}, H_{sj} and K_{sj}
longitudinal transverse distance from the center of gravity of suspension system to the front axis of the suspension system	l_1
pitching angle of the left and right balance bars of the suspension system	φ_{p1} and φ_{p2}
vertical displacement of the $j-th$ axle	z_{uj}
angle of inclination of the $j-th$ wheel shaft	ϕ_{uj}
lateral distance between the left and right springs of the suspension system	b_{s1}, b_{s2} and b_{s3}
damping forces of front suspension left and right springs	F_{d1} and F_{d2}
resultant moment of the cab in the direction of axes X_B, Y_B and Z_B	N_{xb}, N_{yb} and N_{zb}
transverse (longitudinal) distance of cab center of gravity to set 1, set 2 and set 3 bearing spring	l_{17}, l_{18} and l_{19} (l_{22}, l_{23} and l_{24})
transverse (longitudinal) distance of body center of gravity to set 1, set 2 and set 3 tires	l_{25}, l_{26} and l_{27} (l_{28}, l_{29} and l_{30})
transverse distance (longitudinal distance) between the body center of gravity and the cab front (rear) spring	$l_{20}(l_{21})$
longitudinal distance from the center of gravity of the suspension system to the center of gravity of the rear axle of the suspension	l_2

3. Model building

In this paper, the kinematic characteristics of a heavy-duty vehicle are considered to construct a 26 DOF vehicle body and a cab model. As shown in Figs. 1-4, the considered heavy vehicle has one front axle and two rear axles, which is called a three-axial vehicle. The degrees of freedom are vertical, roll and pitch displacements of the diver cab, vehicle body, the vertical and roll motion of three wheel axles, the pitch angles of the left and right balancing pole on rear suspension, and roll angle the of each tire. To further study the coupling property with each part, the vertical, roll and pitch motion of cab and body is modeled independently. Before introducing the related coordinate systems, the Euler's laws of motion is firstly given.

Lemma 3.1. *Observed from an inertial reference frame, the force applied to a rigid body is equal to the product of the mass of the rigid body and the acceleration of the center of mass, i.e.*

$$F^e = ma_c$$

where F^e is the resultant external force of the rigid body, m is the rigid body mass, and a_c is the acceleration of center of mass.

Lemma 3.2. *. The fixed point O (for example, the origin) of an inertial reference frame is set as the reference point. The net external moment applied to the rigid body is equal to the time rate of change of the angular momentum, i.e.*

$$M_O = \frac{dL_O}{dt}$$

where M_O is the is the external torque at point O, $L_O$is the angular momentum at point O.

3.1. Establishing the related coordinate systems

To analyze the motion of heavy-duty vehicle, the corresponding coordinate frames are elaborated to describe the movement of the vehicle and indicated in Fig. 1. The moving coordinate frame $\{B\}$ is fixed to the vehicle's body and is called the body-fixed reference frame. The second coordinate frame $\{C\}$ is fixed to the cab and is called the cab-fixed reference frame. The third coordinate frame $\{E\}$ is fixed to the earth and is called the earth-fixed reference frame. The last coordinate frame $\{T_i\}$ is fixed to the $i-th$, ($i = 1, 2, 3, 4, 5, 6$) tire and is called the tire-fixed reference frame. In this paper, we assume that the body axes X_B, Y_B, Z_B, the tire axes X_{T_i}, Y_{T_i}, and the cab axes X_C, Y_C, Z_C, of heavy vehicle coincide with the principal axes of inertia, which are usually defined as:

- $X_B/X_{T_i}/X_C$ -longitudinal axis (directed from aft of the body/tire/cab to front).
- $Y_B/Y_{T_i}/Y_C$ -transverse axis (directed to right side of body/tire/cab).
- Z_B/Z_C -normal axis (directed from top to bottom).

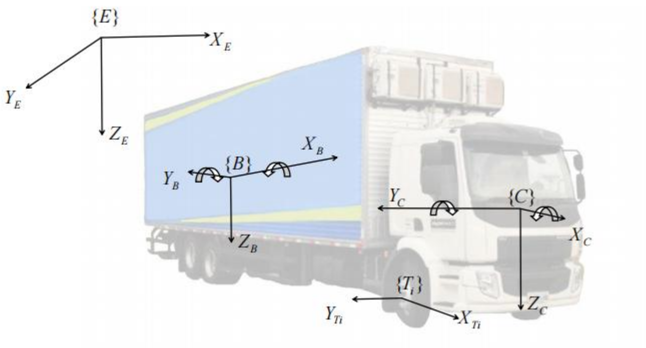

Figure 1. The established reference frame.

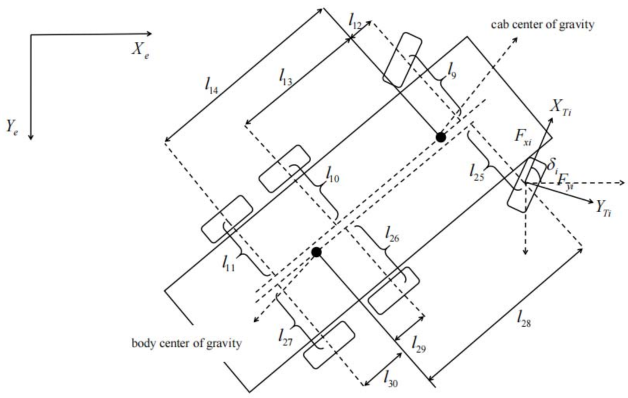

Figure 2. The top view of the three-axle heavy-duty vehicle.

3.2. Analysis of tire motion characteristics

To extract the kinetic model for the considered three-axial heavy-duty vehicle, the coordinate frame T_i is designed for each tire, the corresponding schematic diagram is shown in Fig. 2. By taking the yaw angle into account, the forces produced by the engine are transformed into the forward traction and longitudinal traction on the suspension of heavy-duty vehicle. Based on the coordinate frame and Fig. 2, the forward and lateral traction of each tire can be expressed as

$$\begin{aligned} &F_{Xi} = F_{xi}cos\delta_i - F_{yi}sin\delta_i, \\ &F_{Yi} = F_{yi}sin\delta_i - F_{yi}cos\delta_i, \\ &\dot{\delta_1} = \dot{\delta_2} = \omega_t, \delta_{3,4,5,6} = 0, \\ &i = 1, \cdots, 6. \end{aligned} \tag{3.1}$$

3.3. Analysis of cab motion characteristics

In this subsection, the vertical, roll and pitch motion of the cab are considered to further accurately reflect the performance of spring suspension force between the cab and the body in the actual scenario. In accordance with the coordinate frame $\{C\}$ and Figs. 3-4, the spring force between the cab and body can be given as

$$\begin{aligned} F_{c1} = \; & K_{c1}(-z_c - \varphi_c l_5 - z_b + (\varphi_b - \varphi_0)(l_4 + l_5) - \tfrac{(\phi_b - \phi_c)b_c}{2}) \\ & +H_{c1}(-\dot{z}_c - \dot{\varphi}_c l_5 - \dot{z}_b + \dot{\varphi}_b(l_4 + l_5) - \tfrac{(\dot{\phi}_b - \dot{\phi}_c)b_c}{2}) \end{aligned} \tag{3.2}$$

$$\begin{aligned} F_{c2} = \; & K_{c2}(-z_c - \varphi_c l_5 - z_b + (\varphi_b - \varphi_0)(l_4 + l_5) + \tfrac{(\phi_b - \phi_c)b_c}{2}) \\ & +H_{c2}(-\dot{z}_c - \dot{\varphi}_c l_5 - \dot{z}_b + \dot{\varphi}_b(l_4 + l_5) + \tfrac{(\dot{\phi}_b - \dot{\phi}_c)b_c}{2}) \end{aligned} \tag{3.3}$$

$$\begin{aligned} F_{c3} = \; & K_{c3}(-z_c - \varphi_c l_5 - z_b + (\varphi_b - \varphi_0)(l_4 + l_5) - \tfrac{(\phi_b - \phi_c)b_c}{2}) \\ & +H_{c3}(-\dot{z}_c - \dot{\varphi}_c l_5 - \dot{z}_b + \dot{\varphi}_b(l_4 + l_5) - \tfrac{(\dot{\phi}_b - \dot{\phi}_c)b_c}{2}) \end{aligned} \tag{3.4}$$

$$\begin{aligned} F_{c4} = \; & K_{c4}(-z_c - \varphi_c l_5 - z_b + (\varphi_b - \varphi_0)(l_4 + l_5) + \tfrac{(\phi_b - \phi_c)b_c}{2}) \\ & +H_{c4}(-\dot{z}_c - \dot{\varphi}_c l_5 - \dot{z}_b + \dot{\varphi}_b(l_4 + l_5) + \tfrac{(\dot{\phi}_b - \dot{\phi}_c)b_c}{2}) \end{aligned} \tag{3.5}$$

Furthermore, by viewing the diver cab as a rigid body and employing the **Lemmas 3.1** and **3.2**, the kinematical equation of diver cab model is

$$F_{xc} = m_t(\dot{u}_c - v_c r_c) + m_s(w_c q_c - \dot{q}_c h_{os} - p_c r_c h_{os} - e_{os} q_c^2), \tag{3.6}$$

$$F_{yc} = m_t(\dot{v}_c - u_c r_c) + m_s(\dot{p}_c h_{os} - w_c p_c + q_c(p_c e_{os} - r_c h_{os})) \tag{3.7}$$

$$F_{zc} = m_s(\dot{w}_c + v_c p_c - u_c q_c + h_{os}(q_c^2 + p_c^2) + e_{os}(p_c r_c - \dot{q}_c)), \tag{3.8}$$

$$\begin{aligned} N_{xc} = \; & I_{xxc}\dot{p}_c - I_{xzc}(\dot{r}_c + p_c q_c) + (I_{xxsc} - I_{yysc} - m_s h_{os}^2) q_c r_c \\ & +m_s h_{os}(\dot{v}_c + u_c r_c - w_c p_c), \end{aligned} \tag{3.9}$$

$$\begin{aligned} N_{yc} = \; & I_{yyc}\dot{q}_c - I_{xzc}(p_c^2 - r_c^2) + (I_{yysc} - I_{xxsc}) p_c r_c - m_s h_{os}(\dot{u}_c \\ & -v_c r_c + w_c q_c) - m_s e_{os}(\dot{w}_c + v_c p_c - u_c q_c), \end{aligned} \tag{3.10}$$

$$\begin{aligned} N_{zc} = \; & I_{zzc}\dot{r}_c + I_{xzc}(q_c r_c - \dot{p}_c) + (I_{xxsc} - I_{yysc} + m_s e_{os}^2) p_c q_c \\ & -m_s e_{os} w_c p_c, \end{aligned} \tag{3.11}$$

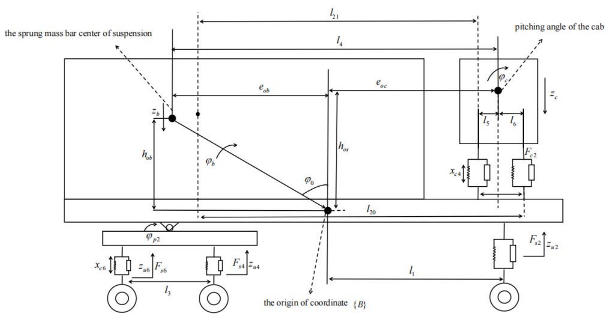

Figure 3. The lateral view of the three-axle heavy-duty vehicle.

When the vehicle is moving, the spring will produce spring force whether it is in a state of compression or tension. However, the direction of the force is opposite, so this paper considers the sign function and the direction of the spring displacement to determine the direction of the spring force. In order to obtain the dynamic force equation of the vehicle cab and body, we assume that the cab and body

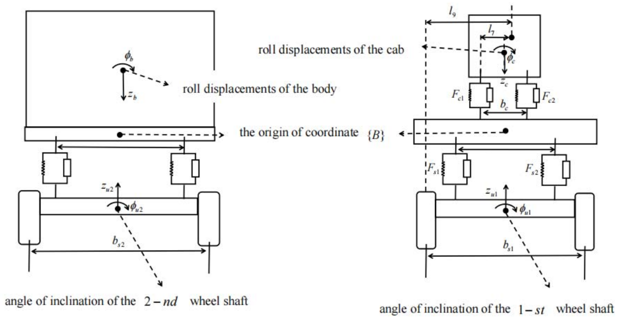

Figure 4. The top view of the three-axle heavy-duty vehicle.

mass are evenly distributed, that is, the transverse distance between the cab and body center of gravity from the left and right tires is the same. By considering the definition of resultant force and resultant moment, the kinetic formula of longitudinal, transverse and vertical forces acting on the cab, as well as the yaw, pitch and roll moments is described as

$$\begin{aligned} F_{xc} = \;& c(\delta_1)c(\varphi_c)\textstyle\sum_{i=1}^{6} F_{Xi} + (s(\phi_c)s(\varphi_c)c(\delta_1) \\ & -s(\delta_1)c(\phi_c))\textstyle\sum_{i=1}^{6} F_{Yi} + (s(\delta_1)s(\phi_c) \\ & +c(\phi_c)s(\varphi_c)c(\delta_1))(F_{c1} + sign(x_{c2})F_{c2} \\ & +sign(x_{c3})F_{c3} + sign(x_{c4})F_{c4}) \end{aligned} \tag{3.12}$$

$$\begin{aligned} F_{yc} = \;& s(\delta_1)c(\varphi_c)\textstyle\sum_{i=1}^{6} F_{Xi} + (s(\phi_c)s(\varphi_c)s(\delta_1) \\ & +c(\delta_1)c(\phi_c))\textstyle\sum_{i=1}^{6} F_{Yi} + (c(\phi_c)s(\phi_c)s(\delta_1) \\ & -c(\delta_1)s(\phi_c))(F_{c1} + sign(x_{c2})F_{c2} \\ & +sign(x_{c3})F_{c3} + sign(x_{c4})F_{c4}) \end{aligned} \tag{3.13}$$

$$\begin{aligned} F_{zc} = \;& -s(\varphi_c)\textstyle\sum_{i=1}^{6} F_{Xi} + (s(\phi_c)c(\varphi_c))\textstyle\sum_{i=1}^{6} F_{Yi} \\ & +(c(\phi_c)c(\varphi_c)(F_{c1} + sign(x_{c2})F_{c2}) \end{aligned} \tag{3.14}$$

$$N_{xc} = (F_{c1} + F_{c2})l_7 - (F_{c3} + F_{c4})l_8, \tag{3.15}$$

$$N_{yc} = (F_{c1} - F_{c2})l_5 + (F_{c3} - F_{c4})l_6, \tag{3.16}$$

$$\begin{aligned} N_{zc} = \;& (F_{X2} - F_{X1})l_9 + (F_{X4} - F_{X3})l_{10} \\ & (F_{X5} - F_{X6})l_{11} + (F_{Y1} + F_{Y2})l_{12} \\ & -(F_{Y3} + F_{Y4})l_{13} - (F_{Y5} + F_{Y6})l_{14}, \end{aligned} \tag{3.17}$$

where $sign(\cdot)$ denotes the symbolic function, $c(\cdot) = cos(\cdot)$ and $s(\cdot) = sin(\cdot)$.

3.4. Analysis of suspension

For the considered heavy duty vehicle, two hydraulic dampers are fixed to the left and right front suspensions, and the balanced suspension does not have any shock absorbers. Thus, to represent the force situation of leaf spring in suspension system, the damping force of the two hydraulic dampers is considered for the front axle. The kinetic equation is given by

$$F_{s1} = K_{s1}(-z_b - (\varphi_b - \varphi_0)l_1 - z_{u1} + \tfrac{(\phi_b-\phi_{u1})b_{s1}}{2}) + F_{d1}, \tag{3.18}$$

$$F_{s2} = K_{s2}(-z_b - (\varphi_b - \varphi_0)l_1 - z_{u1} - \tfrac{(\phi_b-\phi_{u1})b_{s1}}{2}) + F_{d2}, \tag{3.19}$$

$$\begin{aligned} F_{s3} = \;& K_{s3}(-z_b + (\varphi_b - \varphi_0)l_2 - \tfrac{\varphi_{p1}l_3}{2} - z_{u2} + \tfrac{(\phi_b-\phi_{u2})b_{s2}}{2}) \\ & +H_{s3}(-\dot{z}_b + \dot{\varphi}_b l_2 - \tfrac{\dot{\varphi}_{p1}l_3}{2} - \dot{z}_{u2} + \tfrac{(\dot{\phi}_b-\dot{\phi}_{u2})b_{s2}}{2}), \end{aligned} \tag{3.20}$$

$$\begin{aligned} F_{s4} = \;& K_{s4}(-z_b + (\varphi_b - \varphi_0)l_2 - \tfrac{\varphi_{p2}l_3}{2} - z_{u2} + \tfrac{(\phi_b-\phi_{u2})b_{s2}}{2}) \\ & +H_{s4}(-\dot{z}_b + \dot{\varphi}_b l_2 - \tfrac{\dot{\varphi}_{p2}l_3}{2} - \dot{z}_{u2} - \tfrac{(\dot{\phi}_b-\dot{\phi}_{u2})b_{s2}}{2}), \end{aligned} \tag{3.21}$$

$$\begin{aligned} F_{s5} = \;& K_{s5}(-z_b + (\varphi_b - \varphi_0)l_2 - \tfrac{\varphi_{p1}l_3}{2} - z_{u3} + \tfrac{(\phi_b-\phi_{u3})b_{s3}}{2}) \\ & +H_{s5}(-\dot{z}_b + \dot{\varphi}_b l_2 + \tfrac{\dot{\varphi}_{p1}l_3}{2} - \dot{z}_{u3} + \tfrac{(\dot{\phi}_b-\dot{\phi}_{u3})b_{s3}}{2}), \end{aligned} \tag{3.22}$$

$$\begin{aligned} F_{s6} = \;& K_{s6}(-z_b + (\varphi_b - \varphi_0)l_2 - \tfrac{\varphi_{p2}l_3}{2} - z_{u3} + \tfrac{(\phi_b-\phi_{u3})b_{s3}}{2}) \\ & +H_{s6}(-\dot{z}_b + \dot{\varphi}_b l_2 + \tfrac{\dot{\varphi}_{p2}l_3}{2} - \dot{z}_{u3} - \tfrac{(\dot{\phi}_b-\dot{\phi}_{u3})b_{s3}}{2}), \end{aligned} \tag{3.23}$$

3.5. Analysis of body motion characteristics

This is analogous to the diver cab part, taking the body as a rigid body and according to the **Lemmas 3.1 and 3.2**, the force equation of body model can be expressed as

$$F_{xb} = m_t(\dot{u}_b - v_b r_b) + m_b(w_b q_b - \dot{q}_b h_{ob} - p_b r_b h_{ob} - e_{ob} q_b^2), \tag{3.24}$$

$$F_{yb} = m_t(\dot{v}_b - u_b r_b) + m_b(\dot{p}_b h_{ob} - w_b p_b + q_b(p_b e_{ob} - r_b h_{ob})), \tag{3.25}$$

$$F_{zb} = m_b(\dot{w}_b + v_b p_b - u_b q_b) + h_{ob}(q_b^2 + p_b^2) + e_{ob}(p_b r_b - \dot{q}_b)), \tag{3.26}$$

$$\begin{aligned} N_{xb} = \;& I_{xxb}\dot{p}_b - I_{xzb}(\dot{r}_b + p_b q_b) + (I_{xxsb} - I_{yysb} - m_b h_{ob}^2) q_b r_b \\ & + m_b h_{ob}(\dot{v}_b + u_b r_b - w_b p_b), \end{aligned} \tag{3.27}$$

$$\begin{aligned} N_{yb} = \;& I_{yyb}\dot{q}_b - I_{xzb}(p_b^2 - r_b^2) + (I_{yysb} - I_{xxsb}) p_b r_b - m_b h_{ob}(\dot{u}_b \\ & - v_b r_b + w_b q_b) - m_b e_{ob}(\dot{w}_b + v_b p_b - u_b q_b), \end{aligned} \tag{3.28}$$

$$\begin{aligned} N_{zb} = \;& I_{zzb}\dot{r}_b + I_{xzb}(q_b r_b - \dot{p}_b) + (I_{yysb} - I_{xxsb} + m_b e_{ob}^2) p_b q_b \\ & - m_b e_{ob} w_b p_b, \end{aligned} \tag{3.29}$$

Recalling the problem of spring force direction and the assumption of uniform distribution of body mass, the longitudinal, transverse and vertical forces acting on the body are:

$$\begin{aligned} F_{xb} = \;& c(\delta_1)c(\varphi_b)\textstyle\sum_{i=1}^{6} F_{Xi} + (s(\phi_b)s(\varphi_b)c(\delta_1) \\ & - s(\delta_1)c(\phi_b))\textstyle\sum_{i=1}^{6} F_{Yi} + (s(\delta_1)s(\phi_b) \\ & + c(\phi_b)s(\varphi_b)c(\delta_1))(-F_{c1} - sign(x_{c2})F_{c2} \\ & - sign(x_{c3})F_{c3} - sign(x_{c4})F_{c4} + F_{s1} \\ & + sign(z_{u2})F_{s2} + sign(z_{u3})F_{s3} + sign(z_{u4})F_{s4} \\ & + sign(z_{u5})F_{s5} + sign(z_{u6})F_{s6}), \end{aligned} \tag{3.30}$$

$$\begin{aligned} F_{yb} = \;& s(\delta_1)c(\varphi_b)\textstyle\sum_{i=1}^{6} F_{Xi} + (s(\phi_b)s(\varphi_b)s(\delta_1) \\ & + c(\delta_1)c(\phi_b))\textstyle\sum_{i=1}^{6} F_{Yi} + (c(\phi_b)s(\varphi_b)s(\delta_1) \\ & - c(\delta_1)s(\phi_b))(-F_{c1} - sign(x_{c2})F_{c2} \\ & - sign(x_{c3})F_{c3} - sign(x_{c4})F_{c4} + F_{s1} \\ & + sign(z_{u2})F_{s2} + sign(z_{u3})F_{s3} + sign(z_{u4})F_{s4} \\ & + sign(z_{u5})F_{s5} + sign(z_{u6})F_{s6}), \end{aligned} \tag{3.31}$$

$$\begin{aligned} F_{zb} = \;& -s(\varphi_b)\textstyle\sum_{i=1}^{6} F_{Xi} + (s(\phi_b)c(\varphi_b)\textstyle\sum_{i=1}^{6} F_{Yi} \\ & + (c(\phi_b)c(\varphi_b)(-F_{c1} - sign(x_{c2})F_{c2} \\ & - sign(x_{c3})F_{c3} - sign(x_{c4})F_{c4} + F_{s1} \\ & + sign(z_{u2})F_{s2} + sign(z_{u3})F_{s3} + sign(z_{u4})F_{s4} \\ & + sign(z_{u5})F_{s5} + sign(z_{u6})F_{s6}), \end{aligned} \tag{3.32}$$

$$\begin{aligned} N_{xb} = \;& -(F_{c1} + F_{c2})l_{15} + (F_{c3} + F_{c4})l_{16} \\ & + (F_{s1} + F_{s2})l_{17} + (F_{s3} + F_{s4})l_{18} \\ & - (F_{s5} + F_{s6})l_{19}, \end{aligned} \tag{3.33}$$

$$\begin{aligned} N_{yb} = \;& (F_{c2} - F_{c1})l_{20} + (F_{c4} - F_{c3})l_{21} \\ & + (F_{s1} - F_{s2})l_{22} + (F_{s3} - F_{s4})l_{23} \\ & + (F_{s5} - F_{s6})l_{24}, \end{aligned} \tag{3.34}$$

$$\begin{aligned} N_{zb} = \;& (F_{X2} - F_{X1})l_{25} + (F_{X4} - F_{X3})l_{26} \\ & + (F_{X5} - F_{X6})l_{27} + (F_{Y1} + F_{Y2})l_{28} \\ & - (F_{Y3} + F_{Y4})l_{29} - (F_{Y5} + F_{Y6})l_{30}, \end{aligned} \tag{3.35}$$

3.6. Diver cab and body nonlinear model

In this final subsection, a common type of diver cab and body model for heavy-duty vehicle is proposed.

In accordance with 3.1-3.17 and invoking the Euler rotation theorem, the dynamic and kinetic equation of driver cab are designed as

$$\begin{aligned} \dot{\eta}_c &= J_c(\eta_c)\upsilon_c, \\ \dot{\upsilon}_c &= G_c(\eta_c, \upsilon_c)[F_{Xi}^*, F_{Yi}^*]^T + F_c(\upsilon) + u_c, \end{aligned} \tag{3.36}$$

where $\eta_c = [x_c, y_c, z_c, \phi_c, \varphi_c, \delta_1]^T$,

$$J_c(\eta_c) = \begin{bmatrix} J_1(\eta_c) & 0_{3\times3} \\ 0_{3\times3} & J_2(\eta_c) \end{bmatrix},$$

$$J_2(\eta_c) = \begin{bmatrix} 1 & s(\phi_c)t(\varphi_c) & c(\phi_c)t(\varphi_c) \\ 0 & s(\phi_c) & -s(\phi_c) \\ 0 & s(\phi_c)/c(\varphi_c) & c(\phi_c)/c(\varphi_c) \end{bmatrix},$$

$$G_c(\eta_c, \upsilon_c) = \begin{bmatrix} J_3(\eta_c) \\ 0_{3\times2} \end{bmatrix},$$

$$J_3(\eta_c) = \begin{bmatrix} \frac{c(\delta_1)c(\varphi_c)}{m_t} & -s(\delta_1)c(\phi_c) + \frac{s(\phi_c)s(\varphi_c)c(\delta_1)}{m_t} \\ \frac{s(\delta_1)c(\varphi_c)}{m_t} & +c(\delta_1)c(\phi_c) + \frac{s(\phi_c)s(\varphi_c)s(\delta_1)}{m_t} \\ \frac{-s(\varphi_c)}{m_s} & \frac{s(\phi_c)c(\varphi_c)}{m_s} \end{bmatrix},$$

$$F_c(\upsilon_c) = [F_{c1}(\upsilon_c), F_{c2}(\upsilon_c), F_{c3}(\upsilon_c), F_{c4}(\upsilon_c), F_{c5}(\upsilon_c), F_{c6}(\upsilon_c)]^T,$$

$$J_1(\eta_c) = \begin{bmatrix} c(\delta_1)c(\varphi_c) & -s(\delta_1)c(\phi_c) + s(\phi_c)s(\varphi_c)c(\delta_1) & s(\delta_1)s(\phi_c) + c(\phi_c)s(\varphi_c)c(\delta_1) \\ s(\delta_1)c(\varphi_c) & c(\delta_1)c(\phi_c) + s(\phi_c)s(\varphi_c)s(\delta_1) & -c(\delta_1)s(\phi_c) + c(\phi_c)s(\varphi_c)s(\delta_1) \\ -s(\varphi_c) & s(\phi_c)c(\varphi_c) & c(\phi_c)c(\varphi_c) \end{bmatrix},$$

$\upsilon_c = [u_c, v_c, w_c, p_c, q_c, r_c]^T$, $F^*_{Xi} = \sum_{i=1}^6 F_{Xi}$, $F^*_{Yi} = \sum_{i=1}^6 F_{Yi}$,

$u_c = \begin{bmatrix} 0_{5\times1} \\ \frac{((F_{X2}-F_{X1})l_9+(F_{X4}-F_{X3})l_{10}+(F_{X5}-F_{X6})l_{11}}{I_{zzc}} \\ \frac{+(F_{Y1}+F_{Y2})l_{12}-(F_{Y3}+F_{Y4})l_{13}-(F_{Y5}+F_{Y6})l_{14})}{} \end{bmatrix}$, $t(\cdot)$ represents the tangent function. The expansion equation of the matrix $F_c(\upsilon_c)$ is

$$\begin{aligned} F_{c1}(\upsilon_c) = {} & \frac{1}{m_t}[(s(\delta_1)s(\phi_c) + c(\phi_c)s(\varphi_c)c(\delta_1)) * (F_{c1} \\ & +sign(x_{c2})F_{c2} + sign(x_{c3})F_{c3} + sign(x_{c4})F_{c4}) \\ & -m_s(w_cq_c - \dot{q}_ch_{os} - p_cr_ch_{os} - e_{os}q_c^2) + m_tv_cr_c], \end{aligned} \tag{3.37}$$

$$\begin{aligned} F_{c2}(\upsilon_c) = {} & \frac{1}{m_t}[(c(\phi_c)s(\varphi_c)s(\delta) - c(\delta)s(\phi_c)) * (F_{c1} \\ & +sign(x_{c2})F_{c2} + sign(x_{c3})F_{c3} + sign(x_{c4})F_{c4}) \\ & -m_s(\dot{p}_ch_{os} - w_cp_c + q_c(p_ce_{os} - r_ch_{os})) \\ & +m_tu_cr_c], \end{aligned} \tag{3.38}$$

$$\begin{aligned} F_{c3}(\upsilon_c) = {} & \frac{1}{m_s}[c(\phi_c)c(\varphi_c)(F_{c1} + sign(x_{c2})F_{c2} + sign(x_{c3})F_{c3} \\ & +sign(x_{c4})F_{c4})] - (v_cp_c - u_cq_c + h_{os}(q_c^2 + p_c^2) \\ & +e_{os}(p_cr_c - \dot{q}_c)), \end{aligned} \tag{3.39}$$

$$\begin{aligned} F_{c4}(\upsilon_c) = {} & \frac{1}{I_{xxc}}(F_{c1} + F_{c2})l_7 - (F_{c3} + F_{c4})l_8 \\ & -m_sh_{os}(\dot{v}_c + u_cr_c - w_cp_c) + I_{xzc}(\dot{r}_c + p_cq_c) \\ & -(I_{xxsc} - I_{yysc} - m_sh_{os}^2)q_cr_c, \end{aligned} \tag{3.40}$$

$$\begin{aligned} F_{c5}(\upsilon_c) = {} & \frac{1}{I_{yyc}}(I_{xzc}(p_c^2 - r_c^2) - (I_{yysc} - I_{xxsc})p_cr_c \\ & +m_sh_{os}(\dot{u}_c - v_cr_c + w_cq_c) \\ & +m_se_{os}(\dot{w}_c + v_cp_c - u_cq_c) \\ & +(F_{c1} - F_{c2})l_5 + (F_{c3} - F_{c4})l_6), \end{aligned} \tag{3.41}$$

$$\begin{aligned} F_{c6}(\upsilon_c) = {} & \frac{1}{I_{zzc}}[m_se_{os}w_cp_c - I_{xzc}(q_cr_c - \dot{p}_c) \\ & -(I_{yysc} - I_{xxsc} + m_se_{os}^2)p_cq_c], \end{aligned} \tag{3.42}$$

According to kinetic equations (18)-(42) and employing the Euler rotation theorem, the dynamic and kinetic equation of body are designed as

$$\begin{aligned} \dot{\eta}_b &= J_b(\eta_b)\upsilon_b, \\ \dot{\upsilon}_b &= G_b(\eta_b, \upsilon_b)[F^*_{Xi}, F^*_{Yi}]^T + F_b(\upsilon) + u_b, \end{aligned} \tag{3.43}$$

where $\eta_b = [x_b, y_b, z_b\phi_b, \varphi_b, \delta_1]^T$,

$J_b(\eta_b) = \begin{bmatrix} J_1(\eta_b) & 0_{3\times3} \\ 0_{3\times3} & J_2(\eta_b) \end{bmatrix}$, $G_b(\eta_b, \upsilon_b) = \begin{bmatrix} J_3(\eta_b) \\ 0_{3\times2} \end{bmatrix}$,

$\upsilon_b = [u_b, v_b, w_b, p_b, q_b, r_b]^T$, $F^*_{Yi} = \sum_{i=1}^6 F_{Xi}$, $F_b(\upsilon_b) = [F_{b1}(\upsilon_b), F_{b2}(\upsilon_b), F_{b3}(\upsilon_b), F_{b4}(\upsilon_b), F_{b5}(\upsilon_b), F_{b6}(\upsilon_b)]^T$,

$J_2(\eta_b) = \begin{bmatrix} 1 & s(\phi_b)t(\varphi_b) & c(\phi_b)t(\varphi_b) \\ 0 & s(\phi_b) & -s(\phi_b) \\ 0 & s(\phi_b)/c(\varphi_b) & c(\phi_b)/c(\varphi_b) \end{bmatrix}$, $F^*_{Xi} = \sum_{i=1}^6 F_{Xi}$,

$J_3(\eta_b) = \begin{bmatrix} \frac{c(\delta_1)c(\varphi_b)}{m_t} & -s(\delta_1)c(\phi_b) + \frac{s(\phi_b)s(\varphi_b)c(\delta_1)}{m_t} \\ \frac{s(\delta_1)c(\varphi_b)}{m_t} & +c(\delta_1)c(\phi_b) + \frac{s(\phi_b)s(\varphi_b)s(\delta_1)}{m_t} \\ \frac{-s(\varphi_b)}{m_b} & \frac{s(\phi_b)c(\varphi_b)}{m_b} \end{bmatrix}$,

$u_b = \begin{bmatrix} 0_{5\times1} \\ \frac{((F_{X2}-F_{X1})l_{25}+(F_{X4}-F_{X3})l_{26}+(F_{X5}-F_{X6})l_{27}}{I_{zzb}} \\ \frac{+(F_{Y1}+F_{Y2})l_{28}-(F_{Y3}+F_{Y4})l_{29}-(F_{Y5}+F_{Y6})l_{30})}{} \end{bmatrix}$,

$$J_1(\eta_b) = \begin{bmatrix} c(\delta_1)c(\varphi_b) & -s(\delta_1)c(\phi_cb) + s(\phi_b)s(\varphi_b)c(\delta_1) & s(\delta_1)s(\phi_b) + c(\phi_b)s(\varphi_b)c(\delta_1) \\ s(\delta_1)c(\varphi_b) & c(\delta_1)c(\phi_b) + s(\phi_b)s(\varphi_b)s(\delta_1) & -c(\delta_1)s(\phi_b) + c(\phi_c)s(\varphi_b)s(\delta_1) \\ -s(\varphi_b) & s(\phi_b)c(\varphi_b) & c(\phi_b)c(\varphi_b) \end{bmatrix},$$

The expansion equation of the matrix $F_b(\upsilon_b)$ is

$$\begin{aligned} F_{b1}(\upsilon_b) = {} & \frac{1}{m_t}[(s(\delta_1)s(\phi_b) + c(\phi_b)s(\varphi_b)c(\delta_1)) * (-F_{c1} \\ & -sign(x_{c2})F_{c2} - sign(x_{c3})F_{c3} - sign(x_{c4})F_{c4}) \\ & +F_{s1} + sign(z_{u2})F_{s2} + sign(z_{u3})F_{s3} \\ & +sign(z_{u4})F_{s4} + sign(z_{u5})F_{s5} + sign(z_{u6})F_{s6}) \\ & -m_b(w_bq_b - \dot{q}_bh_{ob} - p_br_bh_{ob} - e_{ob}q_b^2) + m_tv_br_b], \end{aligned} \tag{3.44}$$

$$\begin{aligned} F_{b2}(\upsilon_b) = {} & \frac{1}{m_t}[(c(\phi_b)s(\varphi_b)s(\delta) - c(\delta_1)s(\phi_b)) * (-F_{c1} \\ & -sign(x_{c2})F_{c2} - sign(x_{c3})F_{c3} - sign(x_{c4})F_{c4}) \\ & +F_{s1} + sign(z_{u2})F_{s2} + sign(z_{u3})F_{s3} \\ & +sign(z_{u4})F_{s4} + sign(z_{u5})F_{s5} + sign(z_{u6})F_{s6}) \\ & -m_b(\dot{p}_bh_{ob} - w_bp_b + q_b(p_be_{ob} - r_bh_{ob})) \\ & +m_tu_br_b], \end{aligned} \tag{3.45}$$

$$F_{b3}(\upsilon_b) = \frac{1}{m_b}[c(\phi_b)c(\varphi_b)(-F_{c1} - sign(x_{c2})F_{c2} -sign(x_{c3})F_{c3} - sign(x_{c4})F_{c4}) + F_{s1} +sign(z_{u2})F_{s2} + sign(z_{u3})F_{s3} + sign(z_{u4})F_{s4} +sign(z_{u5})F_{s5} + sign(z_{u6})F_{s6}) +m_b(u_b q_b - v_b p_b - h_{ob}(q_b^2 + p_b^2) -e_{ob}(p_b r_b - \dot{q}_b)), \quad (3.46)$$

$$F_{b4}(\upsilon_b) = \frac{1}{I_{xxb}}[(F_{c3} + F_{c4})l_{16} - (F_{c1} + F_{c2})l_{15} +(F_{s1} + F_{s2})l_{17} + (F_{s3} + F_{s4})l_{18} -(F_{s5} + F_{s6})l_{19} + I_{xzb}(\dot{r}_b + p_b q_b) -(I_{xxsb} - I_{yysb} - m_b h_{ob}^2)q_b r_b -m_b h_{ob}(\dot{v}_b + u_b r_b - w_b p_b)], \quad (3.47)$$

$$F_{b5}(\upsilon_b) = \frac{1}{I_{yyb}}[(F_{c2} - F_{c1})l_{20} + (F_{c4} - F_{c3})l_{21} +(F_{s1} - F_{s2})l_{22} + (F_{s3} - F_{s4})l_{23} -(F_{s5} - F_{s6})l_{24} + I_{xzb}(p_b^2 - r_b^2) -(I_{yysb} - I_{xxsb})p_b r_b +m_b h_{ob}(\dot{u}_b - v_b r_b + w_b q_b) +m_b e_{ob}(\dot{w}_b + v_b p_b - u_b q_b)], \quad (3.48)$$

$$F_{b6}(\upsilon_b) = \frac{1}{I_{zzb}}[m_b e_{ob} w_b p_b - I_{xzb}(q_b r_b - \dot{p}_b) -(I_{yysb} - I_{xxsb} + m_b e_{ob}^2)p_b q_b], \quad (3.49)$$

4. Conclusions

In complex working conditions, there is a coupling relationship of the vertical, lateral and longitudinal dynamics of vehicles. By considering the kinetic character of the vertical, roll and pitch motion of the diver cab, vehicle body, the vertical and roll behavior of three wheel axles, the pitch angles of the left and right balancing pole on rear suspension, and roll angle the of each tire. In this paper, a common model of three-axles heavy-duty vehicle with 26 DOF have been proposed to extrude the kinetic characterization diver cab and vehicle body.

Acknowledgment

This work was supported by the National Natural Science Foundation of China under Grants U22A2043 and 62173172.

Conflict of interest

The author declares that there is no conflicts of interest in this paper.

References

1. Y. Lu, S. Yang, S. Li and L. Chen, Numerical and experimental investigation on stochastic dynamic load of a heavy duty vehicle, *Appl. Math. Model.*, **34** (2010), 2698–2710. https://doi.org/10.1016/j.apm.2009.12.006
2. Q. Deng, A general simulation framework for modeling and analysis of heavy-duty vehicle platooning, *IEEE T. Intell. Transp.*, **17** (2016), 3252–3262. 10.1109/TITS.2016.2548502
3. S. Singh, S. Santhakumar, Modeling traffic parameters accounting for platoon characteristics on multilane highways, *Transp. Dev. Econ.*, **69** (2022), 84–96. https://doi.org/10.1007/s40890-022-00166-3
4. M. Sala, F. Soriguera, Macroscopic modeling of connected autonomous vehicle platoons under mixed traffic conditions, *Transportation Research Procedia*, **47** (2020), 163–170. https://doi.org/10.1016/j.trb.2021.03.010
5. Z. Ju, H. Zhang, Y. Tan, Distributed stochastic model predictive control for heterogeneous vehicle platoons subject to modeling uncertainties, *IEEE Intel. Transp. Sy.*, **14** (2022), 25–40.
6. R. Merco, F. Ferrante, P. Pisu, A hybrid controller for DOS-resilient string-stable vehicle platoons, *IEEE T. Intel. Transp.*, **22** (2021), 1697–1707. https://doi.org/10.1109/TITS.2020.29758151
7. L. Xu, W. Zhuang, G. Yin, C. Bian, H. Wu, Modeling and robust control of heterogeneous vehicle platoons on curved roads subject to disturbances and delays, *IEEE T. Veh. Technol.*, **68** (2019), 11551–11564. https://doi.org/10.1109/TVT.2019.2941396
8. Y. Zheng, S. Li, K. Li, F. Borrelli, J. Hedrick, Distributed model predictive control for heterogeneous vehicle platoons under unidirectional topologies, *IEEE*

T. Contr. Syst. T., **25(3)** (2017), 899–910. https://doi.org/10.1109/TCST.2016.2594588

9. J. Zhan, Z. Ma, L. Zhang, Data-driven modeling and distributed predictive control of mixed vehicle platoons, *IEEE Transactions on Intelligent Vehicles*, (2022). https://doi.org/10.1109/TIV.2022.3168591

10. J. Guo, H. Guo, J. Liu, D. Cao, H. Chen, Distributed data-driven predictive control for hybrid connected vehicle platoons with guaranteed robustness and string stability, *IEEE Internet of Things Journal*, **9** (2022), 16308–16321.

11. T. Legouis, A. Laneville, P. Bourassa, G. Payre, Characterization of dynamic vehicle stability using two models of the human pilot behaviour, *Vehicle Syst. Dyn.*, **15** (1986), 1–18. https://doi.org/10.1080/00423118608968837

12. M. Jeleva, B. VilleneuveN. Muralidhar, M. Himabindu, R. Ravikrishna, Modeling of a hybrid electric heavy duty vehicle to assess energy recovery using a thermoelectric generator, *Energy*, **148** (2018), 1046–1059. https://doi.org/10.1016/j.energy.2018.02.023

13. E. Berton, N. Bouaanani, C. Lamarche, N. Roy, Finite element modeling of the impact of heavy vehicles on highway and pedestrian bridge decks, *Procedia Engineering*, **199** (2017), 2451–2456. https://doi.org/10.1016/j.proeng.2017.09.383

14. Y. Yang, H. Wang, G. Xia, Modeling and simulation analysis of wet multi-disk service braking system for heavy vehicles, *IEEE Access*, **8** (2020), 150059–150071. https://doi.org/10.1109/access.2020.3016663

15. Z. Liu, G. Payre, P. Bourassa, Nonlinear oscillations and chaotic motions in a road vehicle system with driver steering control, *Nonlinear Dynamics*, **9** (1996), 281–304. https://doi.org/10.1007/bf01833746

16. Z. Liu, G. Payre, P. Bourassa, Stability and oscillations in a time-delayed vehicle system with driver control, *Nonlinear Dynamics*, **35** (2004), 159–173. https://doi.org/10.1023/b:nody.0000021080.06727.f8

17. L. Serrao, C. Hubert, G. Rizzoni, Dynamic modeling of heavy-duty hybrid electric vehicles, *ASME International Mechanical Engineering Congress and Exposition*, **43106** (2007), 121–128. https://doi.org/10.1115/imece2007-41923

18. H. Ahmadi Jeyed, A. Ghaffari, Modeling and performance evaluation of a heavy-duty vehicle based on the hydraulic power steering system, *Simulation*, **96** (2020), 297–311. https://doi.org/10.1177/0037549719866503

19. S. Li, J. Ren, Driver steering control and full vehicle dynamics study based on a nonlinear three-directional coupled heavy-duty vehicle model, *Math. Probl. Eng.*, **22** (2014), 1–16. https://doi.org/10.1155/2014/352374

20. S. Li, J. Ren, Investigation on three-directional dynamic interaction between a heavy-duty vehicle and a curved bridge, *Adv. Struct. Eng.*, **21** (2018), 721–738. https://doi.org/10.1177/1369433217729516